Fouling control of submerged and side-stream membrane bioreactors based on the statistical analysis of mid-term assays

R. Martínez [a], M.O. Ruiz [a], C. Ramos [a], J.M. Cámara [b], V. Diez [a,*]

[a] Department of Biotechnology and Food Science, Chemical Engineering Division. University of Burgos, Plaza Misael Bañuelos, 09001, Burgos, Spain
[b] Department of Electromechanical Engineering, Electronics Technology Division. University of Burgos, Avda. Cantabria S/n, 09006, Burgos, Spain

ARTICLE INFO

ABSTRACT

The response surface methodology has been applied to study reversible and irreversible fouling rates caused by anaerobic sludge in membrane bioreactors, with the aim of controlling membrane fouling by adjusting filtration conditions. The challenge of obtaining statistically significant results of long-term fouling by means of mid-term assays has been addressed. The individual and combined effects of the filtration flux, backwashing intensity, gas sparging and crossflow velocity on membrane fouling, were analyzed in two types of membranes: an external tubular membrane and a submerged hollow fiber membrane. In the external membrane, the reversible fouling rate was as low as 0.27 ± 0.10 mbar/min, depending mainly on the filtration flux and gas sparging. However, the principal control parameter of the irreversible fouling rate was the crossflow velocity, reaching $2.12 \pm 1.75 \ 10^{12}$ m^{-2} in terms of increase of resistance per cubic meter filtered by square meter of membrane. In the submerged membrane, the irreversible fouling rate was quite lower, 0.78 ± 0.40 mbar/d, despite the reversible fouling rate was higher, 1.26 ± 0.42 mbar/min. In this case, the irreversible fouling depended mainly on the backwashing frequency despite the reversible fouling was more affected by the filtration flux and gas sparging. Hence, the approach used to control the reversible fouling rate does not involve mitigating irreversible fouling on both submerged and external membranes. This study provides a methodological basis for the selection of site-specific operating conditions, under which sustainable operation of membrane bioreactors could be achieved.

1. Introduction

Membrane bioreactors (MBR) combine biological degradation processes of organic matter with complete sludge retention of biomass by membrane filtration, preventing biomass losses and improving effluent quality. However, membrane fouling is still one of the major obstacles that limits their application (Abuabdou et al., 2020). Membrane fouling reduces membrane permeability and increases operating and maintenance costs, including membrane replacement (Chang et al., 2002; Meng et al., 2009). In membrane bioreactor literature, two types of fouling are distinguished, called: reversible and irreversible. From a practical point of view, reversible fouling is considered the fouling contribution that can be removed by relaxation, or backwashing. In contrast, the more strongly attached part, which requires chemical cleaning to be removed, is called irreversible fouling (Judd and Judd, 2011). A better control of both reversible and irreversible fouling would decrease operational costs related to membrane cleaning, thereby making MBRs more competitive in comparison to conventional wastewater treatment plants.

The membrane material and module configuration have a significant impact on the fouling control (Luo et al., 2020; Zhang et al., 2020). Microbial communities, and extracellular polymeric substances (EPS), as the main foulants responsible of the filtration resistance increase (Teng et al., 2019), are strongly affected by the physical properties of the membranes such as roughness, zeta potential or contact angle (Zhang et al., 2020) and membrane hydrophilicity (Huang et al., 2021; Li et al., 2021). The chemical composition of the filtered solution also determines the filtration resistance. It has been reported that the presence of Ca^{2+} increases the specific resistance of alginate solutions (Zhang et al., 2018), and that thermodynamic mechanisms can satisfactorily explain changes in filtration resistance allowing a further optimization of ultrafiltration processes (Long et al., 2021; Wu et al., 2020).

Two membrane bioreactors equipped with hollow fiber membranes, one of them submerged in the biological tank and the other located in a side-stream tank have been studied (Andrade et al., 2014). A lower membrane fouling was observed in the external configuration, as a consequence of the lower suspended solids concentration due to the

Abbreviations

AE	First experimental design with external membrane
AnFMBR	Anaerobic filter membrane bioreactor
AnMBR	Anaerobic membrane bioreactor
AS	First experimental design with submerged membrane
b_0	Intercept coefficient (Eq. (7))
b_i	Linear coefficient of the operating condition X_i (Eq. (7))
b_{ij}	Interaction coefficient of the operating conditions X_i and X_j (Eq. (7))
BBD	Box-Behnken experimental design
BE	Second experimental design with external membrane
BS	Second experimental design with submerged membrane
CFV	Crossflow velocity (m s^{-1})
CV	Coefficient of variation
$(dR_0/dt)_{irr}$	Irreversible fouling rate over time (Eq. (5)) (m^{-1}/d)
$(dR_0/dv)_{irr}$	Irreversible fouling rate per net volume filtered (Eq. (4)) (m^{-2})
$(dTMP_0/dt)_{irr}$	Irreversible fouling rate on initial TMP basis (Fig. 1) (mbar/d)
$(dTMP/dt)_{rev}$	Reversible fouling rate (Fig. 1) (mbar/min)
E	External membrane
EPS	Extracellular Polymeric Substances
J_{bw}	Backwash flux (m^3 m^{-2} s^{-1}; L/m^{2}h)
J_f	Filtration flux (m^3 m^{-2} s^{-1}; L/m^{2}h)
J_{net}	Net flux (Eq. (6)) (m^3 m^{-2} s^{-1}; L/m^{2}h)
MBR	Membrane bioreactor
R_0	Resistance at the beginning of the filtration (Eq. (3)) (m^{-1})
S	Submerged membrane
SGD	Specific gas demand (m^3 m^{-2} h^{-1})
t_{bw}	Backwash time (s)
t_c	Cycle duration (s)
t_f	Filtration time (s)
TMP	Normalized transmembrane pressure (Eq. (1)) (mbar)
TMP_0	Initial transmembrane pressure (Fig. 1) (mbar)
TMP_{bw}	Backwashing transmembrane pressure (mbar)
TMP_T	Transmembrane pressure at temperature T (mbar)
TSS	Total suspended solid (mg/L)
v	Net volume filtered per unit of membrane area (m^3 m^{-2})
X_i	Operating condition i (Eq. (7))
X_j	Operating condition j (Eq. (7))
Y	Estimated fouling rate i (Eq. (7))
μ	Permeate viscosity at the reference temperature (Pa·s)
μ_T	Permeate viscosity at the sludge temperature (Eq. (2)) (Pa·s)

breakdown of flocs and cells by the recirculation pumps. The concentration of suspended solids also decreased in a side-stream tubular membrane with gas sparging (Martínez et al., 2020). However, the release of EPS, and the reduction of the mean particle size of the sludge caused a more severe fouling in the external configuration than in a submerged membrane runed in parallel, using the same sludge and identical filtration conditions.

A proper selection of the operating conditions prevents fouling and improves the economic balance of MBRs. Filtration and backwash flux and duration, relaxation and gas sparging are the main parameters in both fouling control and energy consumption minimization (Liu et al., 2020). It has been observed that backwash flux is slightly more efficient than backwash duration in fouling control of submerged hollow fibers membranes (Zsirai et al., 2012). An automatic adjustment of the relaxation and backwash frequency based on a pre-selected transmembrane pressure (TMP) set-point, instead of setting the duration filtration, has minimized the residual fouling resistance and improved the performance of a pilot scale MBR (Villarroel et al., 2013). Fouling reduces membrane permeability and increases operating and maintenance costs. The combination of the backwash initiation by a TMP set-point and an intermittent gas sparging further improved the productivity of the process (Vera et al., 2016).

Mathematical models of the fouling processes have been developed to optimize the operating conditions of membrane bioreactors (Li and Wang, 2006; Wu et al., 2012). The main limitation of the mathematical models is the site-specificity of fouling behavior and the mandatory calibration of the model parameters for each application. Given that the prediction of fouling evolution by theoretical models entails great difficulty, empirical models should be considered as an alternative to improve the filtration processes in membrane bioreactors. Empirical modeling of complex processes, affected by many independent variables, is a time-consuming task. The analysis of single variables enables the evaluation of their individual effects but not the synergic ones. Response surface methodology is a collection of statistical techniques for empirical modeling of multivariable processes. Between response surface methods, the Box–Behnken experimental designs offer the advantage of requiring fewer test runs than others of similar accuracy.

The potential of Box-Behnken experimental design (BBD) in membrane fouling control has already been proven. BBD notably reduces the required number of experiments of the factorial design, by dividing the experimental range of each variable into three levels and running only those experiments that combine two extreme levels (Box and Behnken, 1960). BBD has been applied to the study of external tubular membranes (Jeison and van Lier, 2006), submerged hollow fibers membranes (Asif et al., 2017; Pourabdollah et al., 2016) and flat-sheet membranes (Fu et al., 2012). External tubular membranes and submerged hollow-fibers membranes commonly used in MBR have been compared under the same conditions (Martínez et al., 2020), but to the best of our knowledge, the effect of the operating parameters in each membrane has not been evaluated. Critical flux (Jeison and van Lier, 2006), TMP increase (Pourabdollah et al., 2016), or specific flux (Fu et al., 2012) have been evaluated as response to characterize fouling. However, the former responses do not take into account all the mechanisms of the fouling process. Critical flux is determined by the reversible fouling, whereas the specific flux or the increase of TMP throughout the experience depend on irreversible fouling. To the best of our knowledge, no previous studies have compared reversible and irreversible fouling rates as fouling indicators.

The aim of this work is therefore to study reversible and irreversible fouling rates in submerged and side-stream membranes, in gas-lift configuration, by evaluating the effect of the filtration and backwash fluxes, filtration and backwash duration, backwash frequency, specific gas demand and, in the case of external membrane, the crossflow velocity. BBDs were used to reduce the number of assays and the duration of the experiment and to avoid sludge alteration throughout the study. The main factors regulating reversible and irreversible fouling rates were identified via standardized effects analyses; furthermore, the sensitivity of the fouling rates to the interactions between different operating conditions was depicted in response surface plots. The challenge of obtaining representative results for long-term irreversible fouling rate from mid-term experimental assays has also been addressed.

2. Materials and methods

2.1. Experimental set-ups

Two filtration set-ups with two different types of ultrafiltration membranes commonly used in membrane bioreactors were used. The

first set-up, (E), was equipped with an external backwashable tubular membrane composed of 13 tubes of 8 mm in diameter and 1 m in length, with a filtration area of 0.31 m^2 (Berghof 63.03I8). The external membrane, made of PVDF with a nominal pore size of 0.04 μm, was operated in gas-lift mode. The other filtration set-up, (S), was equipped with a submerged hollow fiber PVDF membrane, with the same pore size, 0.04 μm, and a filtration area of 0.93 m^2 (ZeeWeed ZW-10). The sludge is placed in two sealed tanks, 20 L in volume. Both set-ups were equiped with compressors (Secoh SV50) for membrane scouring by nitrogen recirculation. Reversible wear pumps (Micropump Eagle Drive GJ-N21) were used for filtration and backwashing. The external membrane set-up was equipped with a low speed vortex pump (Letrin FHW40) for sludge recirculation to maintain the selected crossflow velocity. Digital pressure, flow-meter, and temperature sensors were used for filtration monitoring, and a PLC (M-Duino 42, Industrial Shields) to program the experiments. Further details about the set-ups may be found elsewhere (Martínez et al., 2020).

Anaerobic sludge from an industrial anaerobic digester treating food waste (Ecoalia Group, Burgos, Spain) was used, whose concentration was 60 g TSS/L. Once in the laboratory, the sludge samples were not fed until the daily biogas production was negligible. The sludge was diluted to a concentration of 4.0 g TSS/L with effluent from an anaerobic filter membrane bioreactor, AnFMBR pilot plant treating slaughterhouse wastewater. The selected concentration corresponds to the TSS in the filtration tank of the mentioned AnFMBR, in the range of 3504 ± 311 mg TSS/L (Diez et al., 2021).

Before performing the filtration assays, the membranes were cleaned following a three-step protocol, using sequentially 100 mg/L and 500 mg/L of sodium hypochlorite and 100 mg/L of oxalic acid. Then the membranes were conditioned with the sludge during 24 h under gentle filtration conditions. Filtration and backwash fluxes were of 8 and 14 L/m^{2}h, respectively, for the external membrane, and 12 and 18 L/m^{2}h, for the submerged one, using filtration cycles of 10 min with 30 s for backwashing. The aim of the conditioning period was to exclude the immediate but brief stage of fouling over the first hours of filtration after membrane cleaning, when the increase in resistance was clearly faster than the following linear behavior (Yang et al., 2020; Zsirai et al., 2012).

2.2. Reversible and irreversible fouling

Since the filtration assays were performed at room temperature, before determining fouling rates, to correct the TMP fluctuations due to temperature differences, TMP was normalized to a reference temperature, 30 °C, by means of Eq. (1):

$$TMP = TMP_T \frac{\mu}{\mu_T} \tag{1}$$

where, TMP is the normalized transmembrane pressure at the reference temperature (Pa), μ is the permeate viscosity at that temperature (Pa·s), TMP_T is the experimental transmembrane pressure, and μ_T is the permeate viscosity at the sludge temperature, T (°C), approximately represented by the viscosity of water, determined by Eq. (2) (Wazer et al., 1964):

$$\mu_T = \frac{0.497}{(42.5 + T)^{1.5}} \tag{2}$$

Fig. 1 shows schematically two typical TMP profiles from an experimental run, the reversible fouling rate, $(dTMP/dt)_{rev}$, the initial transmembrane pressure of each filtration cycle, TMP_0, the backwashing transmembrane pressure, TMP_{bw}, and the irreversible fouling rate, $(dTMP_0/dt)_{irr}$, as the increase of TMP_0 throughout the experimental run. To determine the irreversible fouling rate Schoeberl et al. (2005) suggested a minimum filtration time of 7 days, in order to obtain reasonable good linear correlation coefficients ($R^2 = 0.92$). However, it is hard to perform 15–27 such long runs with unchanged biomass. Zsirai et al. (2013) determined the irreversible fouling rate by 15-h filtration tests, which show useful qualitative and comparative information about fouling behavior. In this work TMP_0, $(dTMP/dt)_{rev}$, and $(dTMP_0/dt)_{irr}$, determination has been improved through the use of robust linear regressions method reducing the weight of the outliers that contaminate the slope and intercept estimations of the least squares regression. Huber's method was used with a tuning constant of 1.345 according to the 95% asymptotic efficiency rule (Huber, 1973). In the same way, the average reversible fouling rate in each operating condition has been calculated as the robust mean of $(dTMP/dt)_{rev}$ of the cycles performed in the experimental run. The coefficients of variation (CV) were calculated from the weighted data according to the same robustness criteria.

The resistance at the beginning of the filtration stage, R_0 (m^{-1}), was determined by Darcy's law, Eq. (3):

$$R_0 = \frac{TMP_0}{J_f \cdot \mu} \tag{3}$$

where, J_f is the filtration flux (m^3·m^{-2} s^{-1}).

The irreversible fouling rate was calculated in terms of resistance and on the basis of the net production of permeate per unit of membrane area, according to the productivity of the membrane, dependent on the fluxes and the durations of filtration and backwashing steps (Drews, 2010). For this purpose, the irreversible increase in resistance over the net production of permeate per unit of membrane area, $(dR_0/dv)_{irr}$
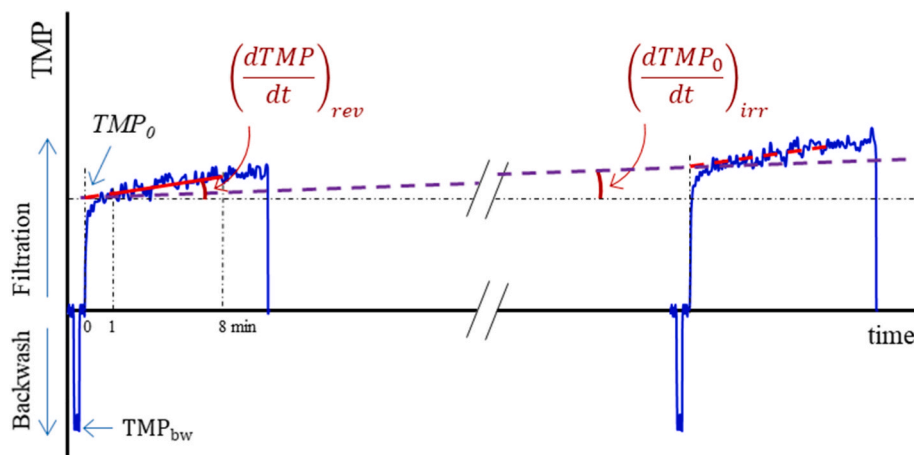

Fig. 1. Normalized transmembrane pressure (TMP) profile at the reference temperature, where TMP_0 is TMP at the beginning of filtration; TMP_{bw} is TMP during backwashing; $(dTMP/dt)_{rev}$ is the reversible fouling rate in each cycle; and, $(dTMP_0/dt)_{irr}$ is the irreversible fouling rate in the experimental run.

(m^{-2}) (Eq. (4)), was determined from the irreversible fouling rate expressed in resistance terms, $(dR_0/dt)_{irr}$ $(m^{-1} \cdot s^{-1})$ (Eq. (5)) and the net flux, J_{net}, $(m^3\ m^{-2}\ s^{-1})$ (Eq. (6)):

$$\left(\frac{dR_0}{dv}\right)_{irr} = \frac{(dR_0/dt)_{irr}}{J_{net}} \tag{4}$$

$$\left(\frac{dR_0}{dt}\right)_{irr} = \left(\frac{dTMP_0}{dt}\right)_{irr} \frac{1}{\mu \cdot J_f} \tag{5}$$

$$J_{net} = \frac{J_f \cdot t_f - J_{bw} \cdot t_{bw}}{t_c} \tag{6}$$

where, v is the net volume filtered per unit of membrane area $(m^3\ m^{-2})$; t_f is the duration of filtration (s); J_{bw} is the backwash flux $(m^3\ m^{-2}\ s^{-1})$; t_{bw} is the duration of backwash (s); and, t_c is the total duration of the filtration cycle (s), sum of filtration, backwash and relaxation steps.

2.3. Box-Behnken experimental design

Four BBDs were used to assess the effect of filtration and backwash fluxes, the duration of both steps, the specific gas demand (SGD), and, in the case of the external membrane, the crossflow velocity (CFV), on both reversible and irreversible fouling rates. In the experimental designs labelled 'A', the variables t_c, J_f, and SGD were studied in both membranes and, in addition, CFV was also studied in the external membrane. In the experimental designs labelled 'B', the operating conditions directly related to backwash, i.e. frequency, t_c, duration, t_{bw}, and strength, J_{bw}, were studied in both membrane set-ups. The operating conditions used in each BBD in the external and submerged membranes are presented in Table 1, where −1, 0, and +1, represent the low, middle, and high levels of each variable. The filtration and backwash fluxes of external membrane were lower than those of the submerged membrane, according to previous results obtained in the comparison of both membranes (Martínez et al., 2020). Crossflow velocity was examined between 0.43 and 0.59 m/s, in the order of the reported for gas-lift AnMBRs, between 0.3 and 1.0 m/s (Prieto et al., 2013).

In the BBDs labelled BE, AS, and BS 15 runs were conducted to study 3 operating conditions, while in the BBD labelled AE, 27 runs were performed to include the CFV as particular operating condition of external membranes. Therefore, the entire duration of the experimental designs was 3.75 days for BE, AS and BS, and 6.75 days for AE, which can be considered relatively short tests with regard to the number of variables and levels studied. The combination of the levels of the operating condition in each run and the statistical analysis of the results were performed using Statgraphics® Centurion XVIII. A two-factor interaction response surface model was used for reversible and irreversible fouling rates with the following polynomial equation (Eq. (7)):

$$Y = b_0 + \sum b_i X_i + \sum b_{ij} X_i X_j \tag{7}$$

where, Y is the estimated fouling rate, either reversible, $(dTMP/dt)_{rev}$, or irreversible, $(dR_0/dv)_{irr}$; b_0 is the corresponding intercept coefficient; b_i

is the linear effect coefficient of the operating condition X_i; and, b_{ij} is the interaction effect coefficient of the operating conditions, X_i and X_j.

3. Results and discussion

3.1. Observed reversible and irreversible fouling rates

The experimental values of the reversible and irreversible fouling rates from the BBDs carried out with both membranes are presented in Table 2. The external membrane operated under very low reversible fouling rates, between 0.07 and 0.55 mbar/min, in the range of those reported for long-term operation of full-scale MBRs in subcritical conditions (Drews, 2010; González et al., 2018). Although the coefficients of variation of $(dTMP/dt)_{rev}$ are apparently high, up to 17.9%. it should be considered that pressure fluctuations due to bubling make difficult to determine such small TMP slopes. Moreover, these deviations were lower than those reported by Le-Clech et al. (2005), 0.17 ± 0.06 mbar/min, using a side-stream tubular membrane operating at a similar CFV.

Despite operating under subcritical conditions, the irreversible fouling rate of the external membrane was really high, reaching values between 0.43 and $7.2 \times 10^{12}\ m^{-2}$, which expressed as daily TMP increase are 3.0–49.8 mbar/d. Those values could be considered normal irreversible fouling rates in lab-scale studies over short time frames, but are above those recommended for long-term operation for full-scale MBR, 1.4–14 mbar/d (Drews, 2010). It is remarkable that the CV of the observed $(dR_0/dv)_{irr}$ of the external membrane were always below 10%, usually between 5% and 7%, which corroborates that robust statistics make possible to obtain a good estimation of irreversible fouling rate in 6-h runs. The irreversible fouling rates in BE BBD were slightly lower than in AE, but a direct comparison of the fouling rates does not allow to distinguish the effect of the tested variables.

The reversible fouling rates in the submerged membrane (Table 3) were between 0.48 and 2.08 mbar/min, around four times higher than in the external membrane. However, the irreversible fouling rate of the submerged membrane was substantially lower, between 0.10 and $1.70 \cdot 10^{12}\ m^{-2}$ that expressed as increase of TMP over time are 3.6–31.8 mbar/d. Despite these values were notably lower than the reported in literature for similar filtration fluxes, between 53 and 96 mbar/d (Zsirai et al., 2013), the irreversible fouling rates reached are still above the advisable for long-term operation of MBRs.

3.2. Standardized effect of the operating conditions and their interactions on fouling

The analysis of the standardized effects makes possible to determine which of the operating conditions studied, or interactions between them, are most significant in the experimental range. The Pareto diagrams were modified to display the standardized effects of each operating condition on reversible and irreversible fouling rates in the same graph (Fig. 2 and Fig. 3), and to compare the significance level of each variable and interaction on both fouling rates. Reference vertical lines

Table 1
Operating conditions of the Box-Behnken experimental designs.

BBD code	External Membrane												Submerged Membrane											
	AE			BE									AS			BS								
Level	−1	0	+1	−1	0	+1							−1	0	+1	−1	0	+1						
t_c (min)	10	15	20	10	15	20							10	15	20	10	15	20						
J_f (L/m^{2}h)	11	12	13		12								18	20	22		20							
J_{bw} (L/m^{2}h)		20		20	25	30								30		27	30	33						
SGD (m^3/m^{2}h)	1.2	1.3	1.4		1.3								1.2	1.3	1.4		1.3							
t_{bw} (s)		30		20	30	40								30		20	30	40						
CFV (m/s)	0.43	0.51	0.59		0.51									n/a			n/a							

t_c: cycle duration; J_f: filtration flux; J_{bw}: backwash flux; SGD: specific gas demand; t_{bw}: backwash duration; CFV: crossflow velocity; BBD Box-Behnken design; AE and BE: experimental designs with external membrane; AS and BS: experimental designs with the submerged membrane; n/a: not applicable.

Table 2
Reversible and irreversible fouling rates of external membrane runs.

AE

Level				$(dTMP/dt)_{rev}$ (mbar/min)	CV	$(dR_0/dv)_{irr}$ (10^{12} m^{-2})	CV
t_c,	J_f,	SGD,	CFV				
0	0	0	0	0.19	14.4%	4.0	6.9%
−1	−1	0	0	0.25	12.0%	1.5	6.5%
+1	−1	0	0	0.17	7.9%	1.2	3.9%
−1	+1	0	0	0.33	6.3%	4.5	3.3%
+1	+1	0	0	0.32	10.3%	4.5	3.6%
0	0	−1	−1	0.39	6.1%	4.1	4.9%
0	0	+1	−1	0.22	15.9%	5.2	3.9%
0	0	−1	+1	0.42	5.5%	1.4	3.8%
0	0	+1	+1	0.11	16.2%	0.5	5.0%
−1	0	0	−1	0.27	16.9%	7.2	4.1%
+1	0	0	−1	0.32	11.6%	2.5	5.9%
−1	0	0	+1	0.33	10.3%	1.0	5.9%
+1	0	0	+1	0.26	9.5%	1.1	6.3%
0	0	0	0	0.26	7.3%	1.2	3.0%
0	−1	−1	0	0.23	7.1%	1.4	4.4%
0	+1	−1	0	0.42	4.4%	4.5	3.6%
0	−1	+1	0	0.21	17.9%	0.5	4.8%
0	+1	+1	0	0.32	10.3%	4.1	4.6%
−1	0	−1	0	0.38	4.9%	1.5	4.3%
+1	0	−1	0	0.28	5.6%	1.5	3.1%
−1	0	+1	0	0.34	7.7%	1.1	4.2%
+1	0	+1	0	0.15	14.8%	2.9	3.7%
0	−1	0	−1	0.22	10.8%	4.1	4.7%
0	+1	0	−1	0.34	12.5%	6.3	4.0%
0	−1	0	+1	0.28	9.2%	1.2	9.9%
0	+1	0	+1	0.32	6.2%	0.9	4.6%
0	0	0	0	0.23	9.7%	1.2	4.5%

BE

Level			$(dTMP/dt)_{rev}$ (mbar/min)	CV	$(dR_0/dv)_{irr}$ (10^{12} m^{-2})	CV
t_c,	t_{bw},	J_{bw}				
0	0	0	0.19	9.2%	1.03	5.3%
−1	−1	0	0.08	7.9%	0.43	6.3%
+1	−1	0	0.12	11.2%	1.13	5.3%
−1	+1	0	0.36	5.4%	0.44	5.9%
+1	+1	0	0.36	12.3%	0.44	9.2%
−1	0	−1	0.19	8.1%	0.46	5.7%
+1	0	−1	0.14	5.5%	0.54	5.0%
0	0	0	0.22	4.7%	1.66	6.7%
−1	0	+1	0.44	10.3%	1.29	6.4%
+1	0	+1	0.32	7.5%	1.08	6.5%
0	−1	−1	0.07	6.5%	0.45	6.7%
0	+1	−1	0.17	7.9%	1.94	7.8%
0	−1	+1	0.26	14.5%	3.38	5.4%
0	+1	+1	0.55	12.2%	1.02	6.4%
0	0	0	0.17	7.2%	2.51	5.3%

t_c: cycle duration; J_f: filtration flux; J_{bw}: backwash flux; SGD: specific gas demand; t_{bw}: backwash duration; CFV: crossflow velocity; $(dTMP/dt)_{rev}$: reversible fouling rate; $(dTMP_0/dt)_{irr}$: irreversible fouling rate; CV: coefficient of variation; AE and BE: Box-Benhnken designs with the external membrane.

Table 3
Reversible and irreversible fouling rates in submerged membrane runs.

AS

		Level	$(dTMP/dt)_{rev}$ (mbar/min)	CV	$(dR_0/dv)_{irr}$ ($\times 10^{12}$ m^{-2})	CV
t_c,	J_f,	SGD				
0	0	0	0.87	12.6%	0.11	0.6%
−1	−1	0	0.67	21.5%	0.12	4.7%
+1	−1	0	0.48	22.0%	1.15	16.5%
−1	+1	0	1.28	37.8%	0.50	3.7%
+1	+1	0	1.89	20.5%	1.13	45.3%
−1	0	−1	1.17	15.4%	0.47	3.2%
+1	0	−1	1.27	16.2%	1.16	13.1%
0	0	0	0.83	16.2%	1.24	44.0%
−1	0	+1	1.19	31.1%	0.50	0.5%
+1	0	+1	0.60	18.6%	0.69	58.9%
0	−1	−1	0.72	16.6%	0.58	37.6%
0	+1	−1	2.04	27.1%	0.86	1.9%
0	−1	+1	0.81	20.5%	0.77	4.9%
0	+1	+1	0.87	20.0%	0.46	7.6%
00	0		1.38	10.4%	0.36	51.5%

BS

		Level	$(dTMP/dt)_{rev}$ (mbar/min)	CV	$(dR_0/dv)_{irr}$ ($\times 10^{12}$ m^{-2})	CV
t_c,	J_{bw},	t_{bw}				
0	0	0	1.57	6.0%	0.88	6.0%
−1	−1	0	1.24	7.6%	0.99	9.0%
+1	−1	0	1.31	10.5%	0.66	7.5%
−1	+1	0	1.87	13.4%	0.23	4.6%
+1	+1	0	1.71	13.1%	1.70	8.3%
−1	0	−1	1.22	8.2%	0.81	4.9%
+1	0	−1	1.19	7.3%	1.29	7.3%
0	0	0	1.25	12.2%	0.88	7.3%
−1	0	+1	1.71	6.7%	0.50	8.2%
+1	0	+1	1.43	13.8%	1.16	12.5%
0	−1	−1	1.02	7.6%	1.51	6.0%
0	+1	−1	1.45	11.9%	0.41	6.1%
0	−1	+1	1.32	14.0%	0.90	9.6%
0	+1	+1	2.08	14.5%	0.52	6.1%
0	0	0	1.25	11.2%	0.80	4.4%

AS: experimental design A with submerged membrane; BS: experimental design B with submerged membrane. t_c: cycle duration, J_f: filtration flux, J_{bw}: backwash flux, SGD: specific gas demand, t_{bw}: backwash duration, $(dTMP/dt)_{rev}$: reversible fouling rate, $(dR_0/dv)_{irr}$: irreversible fouling rate, CV:coefficient of variation.

on these diagrams allow assessing which variables or interactions have statistically significant effects, with a 95% confidence level. The signs (+) and (−) indicate whether the fouling rate increases with the variable within the range studied, "positive effect"; or the fouling rate decreases when the variable increases, "negative effect".

The duration of filtration cycle, filtration flux, and specific gas demand all had significant effects on the reversible fouling rate in the external membrane (Fig. 2 – AE). $(dTMP/dt)_{rev}$ increased with J_f, and decreased with t_c and SGD. It is noteworthy that CFV had no statistically significant effect on $(dTMP/dt)_{rev}$, due to the greater effect of gas-sparging, distinctive of gas-lift configuration, and the low filtration flux, with regard to conventional side-stream MBRs. This finding is in agreement with a study of the reversible fouling in a tubular membrane that verified that the increase in superficial gas velocity had a greater effect on the fouling control than the increase of CFV (Le-Clech et al., 2005). Furthermore, the effect of backwashing frequency on $(dTMP/dt)_{rev}$ was also noteworthy. It was proved that the decrease in t_c caused an increase of the reversible fouling rate. The BE experimental design corroborated that backwash intensity, especially the increase in backwash flux and duration, caused a statistically significant increase of $(dTMP/dt)_{rev}$. As discussed below, the same behavior was observed in the submerged membrane.
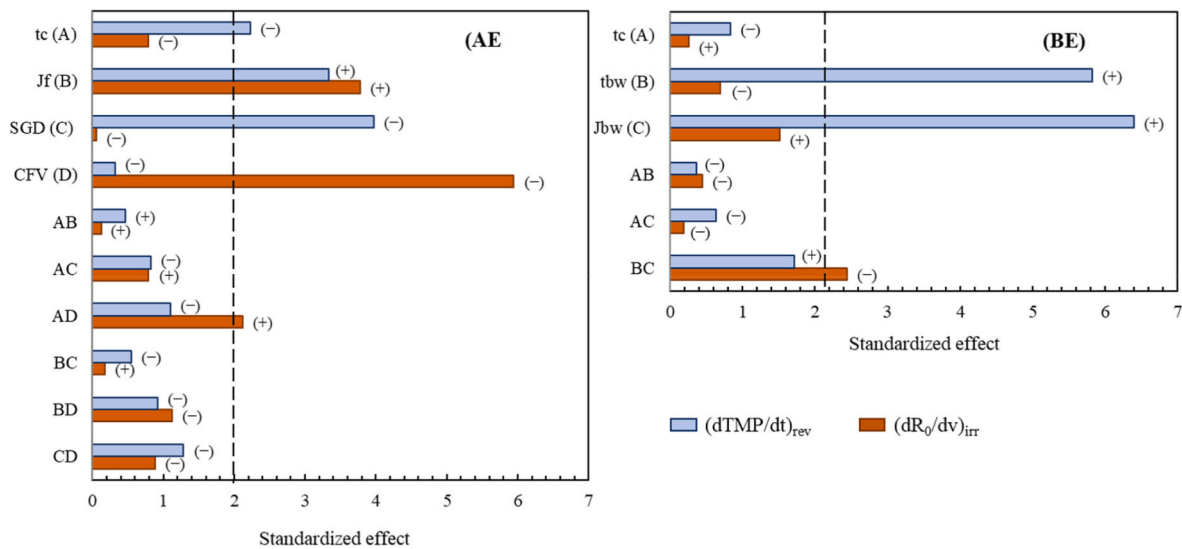
Fig. 2. Standardized effect of the operating condition studied in Box-Behnken designs AE and BE performed with the external membrane. t_c: cycle duration; J_f: filtration flux; SGD: specific gas demand; CFV: crossflow velocity; t_{bw}: backwash duration; J_{bw}: backwash flux, $(dTMP/dt)_{rev}$: reversible fouling rate; $(dR_0/dv)_{irr}$: irreversible fouling rate.
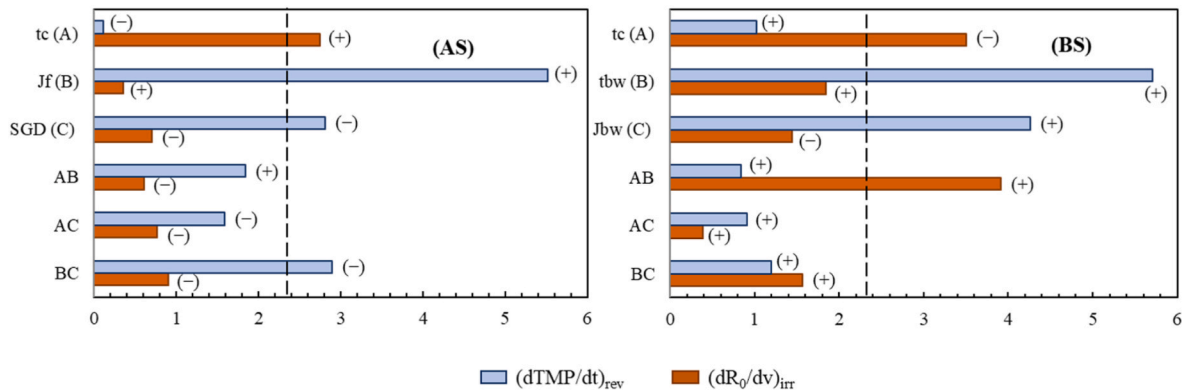

Fig. 3. Standardized effect of the operating condition studied in Box-Behnken designs AS and BS carried out with the submerged membrane. t_c: cycle duration; J_f: filtration flux; SGD: specific gas demand; t_{bw}: backwash duration; J_{bw}: backwash flux; $(dTMP/dt)_{rev}$: reversible fouling rate; $(dR_0/dv)_{irr}$: irreversible fouling rate.

The operating conditions with the highest statistical significance on $(dR_0/dv)_{irr}$ for the external membrane were J_f, and particularly CFV, despite having no significant effect on the reversible fouling. On the contrary, the parameter showing the highest impact on $(dTMP/dt)_{rev}$, SGD, had the lowest standardized effect on $(dR_0/dv)_{irr}$. Backwash frequency, flux and duration, separately, had no statistically significant effects on $(dR_0/dv)_{irr}$ within the range of the BE BBD. However, Fig. 2 – BE shows that the product $J_{bw} \cdot t_{bw}$, i.e. the volume of permeate used for backwashing, lowered the irreversible fouling rate with a confidence level of 95%.

In the submerged membrane, J_f, SGD and their interaction, $J_f \cdot$SGD, were the operating conditions with higher effects on $(dTMP/dt)_{rev}$ (Fig. 3 – AS). The reversible fouling rate decreased with SGD, and, according to the negative sign of the standardized effect of the interaction $J_f \cdot$SGD, the controlling effect of SGD on $(dTMP/dt)_{rev}$ is more pronounced for the higher fluxes. It has been reported that the relative reversible fouling rate under sustainable operating conditions increases with filtration flux regardless of SGD, and similarly, the effect of SGD on the relative fouling rate is independent of filtration flux, except in the proximity of the critical flux (Nywening and Zhou, 2009). However, it should be considered that the highest filtration flux used with the submerged membrane, 22 L/m²h, was clearly over the critical flux, with a mean $(dTMP/dt)_{rev}$ of 1.65 ± 0.42 mbar/min.

The effect of backwash intensity on $(dTMP/dt)_{rev}$ in the submerged membrane is shown in Fig. 3 – BS. It is observed that the reversible fouling rate also increased with backwash flux and duration, as in the case of the external membrane. These results cannot be explained by an increase in the convective transport of suspended materials from the bulk mixed liquor, showing the complexity of the fouling processes. This behavior has been related to the recompression process in the external fouling layer, which is not dispersed away from the membrane, suggesting that the compressibility of the fouling layer has a significant contribution on $(dTMP/dt)_{rev}$ (Diez et al., 2021; Vera et al., 2015). Thus, after backwashing, a faster increase in TMP was observed due to cake rearrangement and colloidal entrapment, rather than to the reversible deposition of new particles. According to this finding, after removing pore blocking via backwashing, longer relaxation period with gas scouring should be considered to favor the detachment of the loosened materials. The relaxation time should be determined for each sludge and bioreactor, optimal relaxation times of up to 4 min have been reported for flat sheet membranes (Christensen et al., 2016).

In the submerged membrane, the effect of t_c on $(dR_0/dv)_{irr}$ was higher than the effect of either J_f or SGD, which were not statistically significant (Fig. 3 – AS). Table 3 shows the significant increase in irreversible fouling caused by the decrease of the backwashing frequency. Severe fouling effects for longer filtration time (more than 12 min) have

been previously reported suggesting that cake consolidation slowed down when filtration frequency increases (González et al., 2018). Cake consolidation over the filtration time could be due to the deformation and rearrangement of foulant particles (Foley, 2006; Jeison and van Lier, 2007), lowering the cake porosity that becomes more prone to entrap colloidal material (Wu et al., 2012). Finally, the analysis of the standardized effects of flux and backwash duration showed no statistically significant impact on $(dR_0/dv)_{irr}$ in the submerged membrane (Fig. 3 - BS), which in turn implies that consolidation effects associated to the filtration time are hardly reverted by the backwashing.

3.3. Response surface diagrams of reversible and irreversible fouling rates

Tables 4 and 5 show the intercepts and coefficients of the polynomial model (Eq. (7)) that allows quantification of the effects of the operating conditions on the reversible and irreversible fouling rates, in the experimental range. A regression of the responses calculated from the polynomial models, and the experimental fouling rates are presented in Fig. 4, accompanied by a 1:1 dashed line to assess the quality of the adjustments. The correlation coefficients were in the range of 0.530–0.908 that can be considered in line with the intrinsic complexity of the fouling processes and the challenge of assessing the irreversible fouling rate in mid-term assay. The regression coefficients were appreciably lower than the reported by Zhang et al. (2014), between 0.904 and 0.908, using Box-Behnken response surface methodology. However, two important differences should be considered. Firstly, in the aforementioned study a new membrane was used for each series of experiments and, secondly, the permeability loss was studied after each filtration run using deionized water, i.e. only one measure of irreversible fouling was taken. It is important to take into account the difficulty of obtaining long-term projection of mid-term effects in continuous assays for the evaluation of the combined effects of three or more variables, even using optimized experimental designs (Zsirai et al., 2013).

Fig. 5 presents the three-dimensional response surfaces of the effect of operating conditions on external membrane fouling (a-d), and on submerged membrane fouling (e-h). The reversible and the irreversible fouling rates obtained in the same experimental design can be compared by rows, and those obtained in different experimental designs can be compared by columns for the reversible fouling rate (a, c, e, g), and for the irreversible fouling rate (b, d, f, h).

The reversible fouling rate of the external membrane, Fig. 5 (a) and (c), was clearly lower than that of the submerged membrane, Fig. 5 (e) and (g), as consequence of the difference in filtration fluxes, 12 ± 1 L/m^2h and 20 ± 2 L/m^2h, respectively. It should be highlighted that in a previous work, using the same filtration fluxes in both membranes, 15 L/m^2h, it was proved that $(dTMP/dt)_{rev}$ of the external membrane was up to twice the $(dTMP/dt)_{rev}$ of the submerged membrane (Martínez et al., 2020). Despite that, the excessive irreversible fouling rate of the external membrane it was not possible to maintain that filtration flux for more than 4 days, which justify the current flux selection. By comparing the reversible fouling rate of the external membrane in AE and BE BBDs, Fig. 5 (a) and (c), it may be noted that J_f and CFV have a lower effect, on $(dTMP/dt)_{rev}$ than J_{bw} and t_{bw}. Unexpectedly, a small increase of the reversible fouling rate with backwashing intensity was observed in Fig. 5 (c). This effect also was observed in the submerged membrane.

The effects of J_f and CFV on the irreversible fouling rate of the external membrane were very pronounced, Fig. 5 (b). CFV was effective in $(dR_0/dv)_{irr}$ control at any filtration flux. In fact, a relatively small increase in CFV from 0.43 to 0.59 m/s allowed the reduction of irreversible fouling rate to approximately a fifth of its value. In the external membrane, backwashing intensity does not have the same effect on the irreversible fouling rate than on the reversible one. Fig. 5 (d) shows that an increase in t_{bw} is only effective on irreversible fouling control for the higher backwashing flux. However, lengthening the backwashing time has detrimental effects when the backwashing flux is insufficient to detach the reversible cake layer. The protective effect of the cake layer facing the internal fouling by macromolecules, and the deterioration of the quality of the backwashing water by humic substances condensation have been pointed out as possible causes of the negative effect of the backwash in the irreversible fouling (Diez et al., 2012; Wu et al., 2008). Therefore, frequent backwashing provides additional opportunities for pore blocking, and the release of EPS caused by the shear conditions of the external membrane could explain the negative effect of backwashing on $(dR_0/dv)_{irr}$.

In the submerged membrane, the effect of SGD on $(dTMP/dt)_{rev}$ depended on filtration flux, Fig. 5 (e). SGD hardly has effect on $(dTMP/dt)_{rev}$ at the lower filtration flux. However, as filtration flux increases, the alleviating effect of scouring on the reversible fouling rate became progressively more important. It is noteworthy that for the highest flux, it was possible to reduce the reversible fouling rate from 2.0 to 1.0 mbar/min by increasing SGD from 1.2 to 1.4 m^3/m^2h. The effect of backwashing intensity on the reversible fouling rate in the submerged membrane, Fig. 5 (g), was similar, even more pronounced, than in the external membrane, and a significant increase of $(dTMP/dt)_{rev}$ with J_{bw} and t_{bw} was observed. This TMP increase after an intense backwash, faster than expected, could be explained by the rearrangement and compression of the loosened material and, therefore, it should be differentiated from the transport and incorporation of new materials from the bulk suspension. The effects of J_f and SGD on irreversible fouling, on the submerged membrane, Fig. 5 (f), presented the same trend as on reversible one. Some decrease in $(dR_0/dv)_{irr}$ with SGD can be appreciated for the higher filtration fluxes whereas for the lower filtration fluxes, increasing SGD had no beneficial effect on $(dR_0/dv)_{irr}$. It has been previously reported that high levels of gas sparging have a low contribution in fouling amelioration for low net fluxes, so the operating cost can be lowered by a reduction in the SGD to the minimum (Schoeberl et al., 2005).

Fig. 5 (h) shows that backwash intensity had a slight impact on $(dR_0/dv)_{irr}$ in the submerged membrane. It is necessary to consider that, in the experimental conditions of the submerged membrane, particularly for TMP below 120 mbar, the cake layer never became overly cohesive. It has been reported that, for TMP in the range of 100–300 mbar and high irreversible fouling rates, around 100 mbar/day, the increase in backwash volume lead to a reduction of the irreversible fouling rate (Zsirai et al., 2012). This newly reflects the cross effects of the operating conditions on the fouling process and justifies the interest of analyzing the control of fouling in a multivariable context. Finally, by comparing the Fig. 5 (e) and (f), and especially the Fig. 5 (g) and (h), it is worth highlighting that the strategy used for the control of the reversible fouling rate is not directly transferable to the control of the irreversible

Table 4
Model parameters (Eq. (7)) for the reversible fouling-rate estimation $(dTMP/dt)_{rev}$.

BBD	b_0	t_c	t_{bw}	J_f	J_{bw}	SGD	CFV	$t_c \cdot J_f$	$t_c \cdot$SGD	$t_c \cdot$CFV	$t_c \cdot t_{bw}$	$t_c \cdot J_{bw}$	$t_{bw} \cdot J_{bw}$	$J_f \cdot$SGD	$J_f \cdot$CFV	SGD$\cdot$CFV
AE	−7.56	0.06	–	0.37	–	4.08	10.50	0.003	−0.005	−0.008	–	–	–	−0.15	−0.31	−4.38
BE	−0.42	0.03	−0.003	–	0.004	–	–	–	–	–	−0.001	−0.001	0.001	–	–	–
AS	−42.02	0.05	–	1.96	–	34.51	–	0.02	−0.35	–	–	–	–	−1.57	–	–
BS	−1.64	0.2	0.007	–	0.07	–	–	–	–	–	−0.002	−0.01	0.002	–	–	–

b_0: corresponding intercetp coefficient; t_c: cycle duration; t_{bw}: backwash duration; J_f: filtration flux; J_{bw}: backwash flux; SGD: specific gas demand; CFV: crossflow velocity; BBD: Box Behnken design; AE and BE: experimental designs with external membrane; AS and BS: Box-Benhnken designs with submerged membrane.

Table 5
Model parameters (Eq. (7)) for the irreversible fouling rate estimation $(dR_0/dv)_{irr}$.

BBD	b_0	t_c	t_{bw}	J_f	J_{bw}	SGD	CFV	$t_c{\cdot}J_f$	$t_c{\cdot}SGD$	$t_c{\cdot}CFV$	$t_c{\cdot}t_{bw}$	$t_c{\cdot}J_{bw}$	$t_{bw}{\cdot}J_{bw}$	$J_f{\cdot}SGD$	$J_f{\cdot}CFV$	$SGD{\cdot}CFV$
AE	−30.03	−2.93	–	3.76	–	6.21	107.2	0.02	0.90	3.00	–	–	–	1.00	−7.94	−62.5
BE	−19.37	0.47	0.56	–	0.71	–	–	–	–	–	−0.003	−0.01	−0.002	–	–	–
AS	−26.69	0.59	–	1.13	–	17.69	–	−0.01	−0.25	–	–	–	–	−0.74	–	–
BS	11.95	−0.53	−0.35	–	−0.22	–	–	–	–	–	0.02	0.005	0.005	–	–	–

b_0: corresponding intercetp coefficient; t_c: cycle duration; t_{bw}: backwash duration; J_f: filtration flux; J_{bw}: backwash flux; SGD: specific gas demand; CFV: crossflow velocity; BBD: Box-Behnken design; AE and BE: experimental designs with external membrane; AS and BS: Box-Behnken designs with submerged membrane.
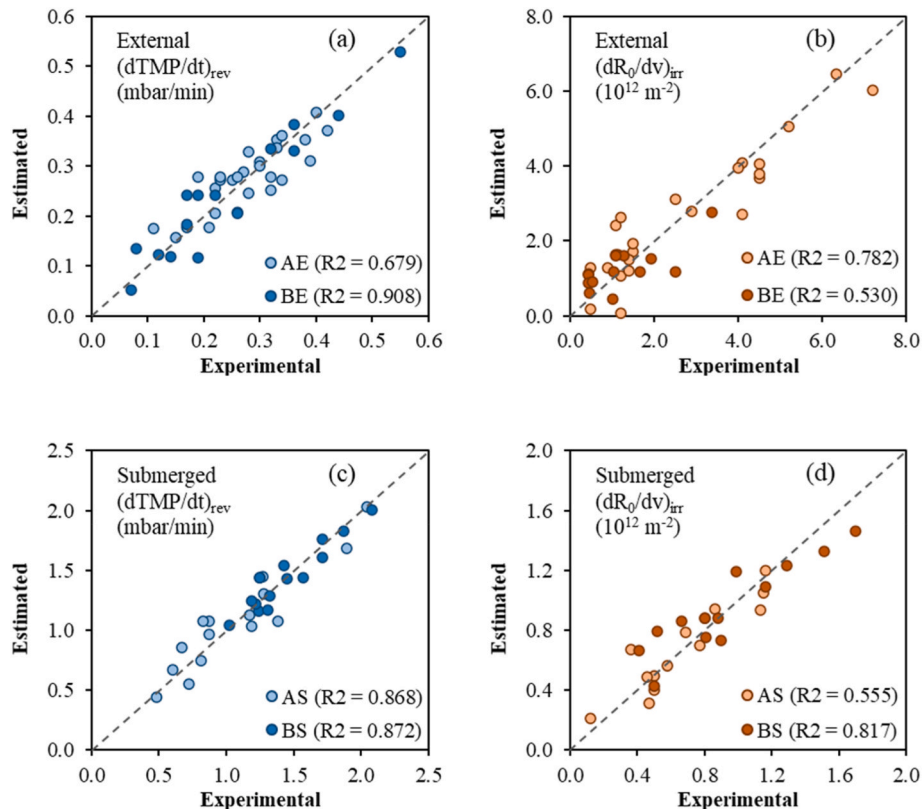
Fig. 4. Estimated results fitted by modeling the experimental results both for reversible, $(dTMP/dt)_{rev}$, and for irreversible, $(dR_0/dv)_{irr}$. fouling rates. (a) reversible and (b) irreversible fouling rates from Box-Behnken designs AE and BE; (c) reversible and (d) irreversible fouling rates from Box-Behnken designs AS and BS.

fouling rate.

4. Conclusions and prospects

The influence of filtration flux, backwash flux, frequency and duration, specific gas demand, and crossflow velocity on reversible and irreversible fouling rates has been evaluated both in an external tubular membrane with gas sparging, and in a submerged hollow-fiber membrane.

Despite the complexity of the fouling process makes difficult to obtain a predictive model of membrane fouling, a statistical analysis allows recognizing the relevance of the effects of the operating parameters. Box–Behnken experimental design has proven to be suitable for comparative analysis of the combined effects of the key filtration parameters in mid-term experiments.

Although the reversible fouling rate of the external membrane was lower than the one of the submerged membrane, its irreversible fouling rate was notably higher. The factors that effectively control the reversible fouling rate were not equally helpful in the control of the irreversible one.

An unexpected increase of $(dTMP/dt)_{rev}$ with the frequency, flux, and duration of backwash on reversible fouling rate was observed in both membranes due to the loosening without detachment of part of the foulants.

Whereas site-specific fouling processes cannot by described by mathematical models, new efforts focused on statistical analysis of short-term test performed in situ will help to establish the optimal operating conditions of large-scale MBRs. Lastly, it will be necessary to establish new fouling indicators, beyond the reversible fouling rate, which should include the fouling layer consolidation as key factor of fouling irreversibility.

CRediT authorship contribution statement

R. Martínez: Investigation, Validation, Formal analysis, Visualization, Writing – review & editing. **M.O. Ruiz:** Validation, Formal analysis, Visualization, Writing – original draft. **C. Ramos:** Methodology, Resources, Visualization, Writing – original draft. **J.M. Cámara:** Software, Validation, Data curation. **V. Diez:** Conceptualization, Methodology, Supervision, Writing – review & editing, Project administration.

Declaration of competing interest

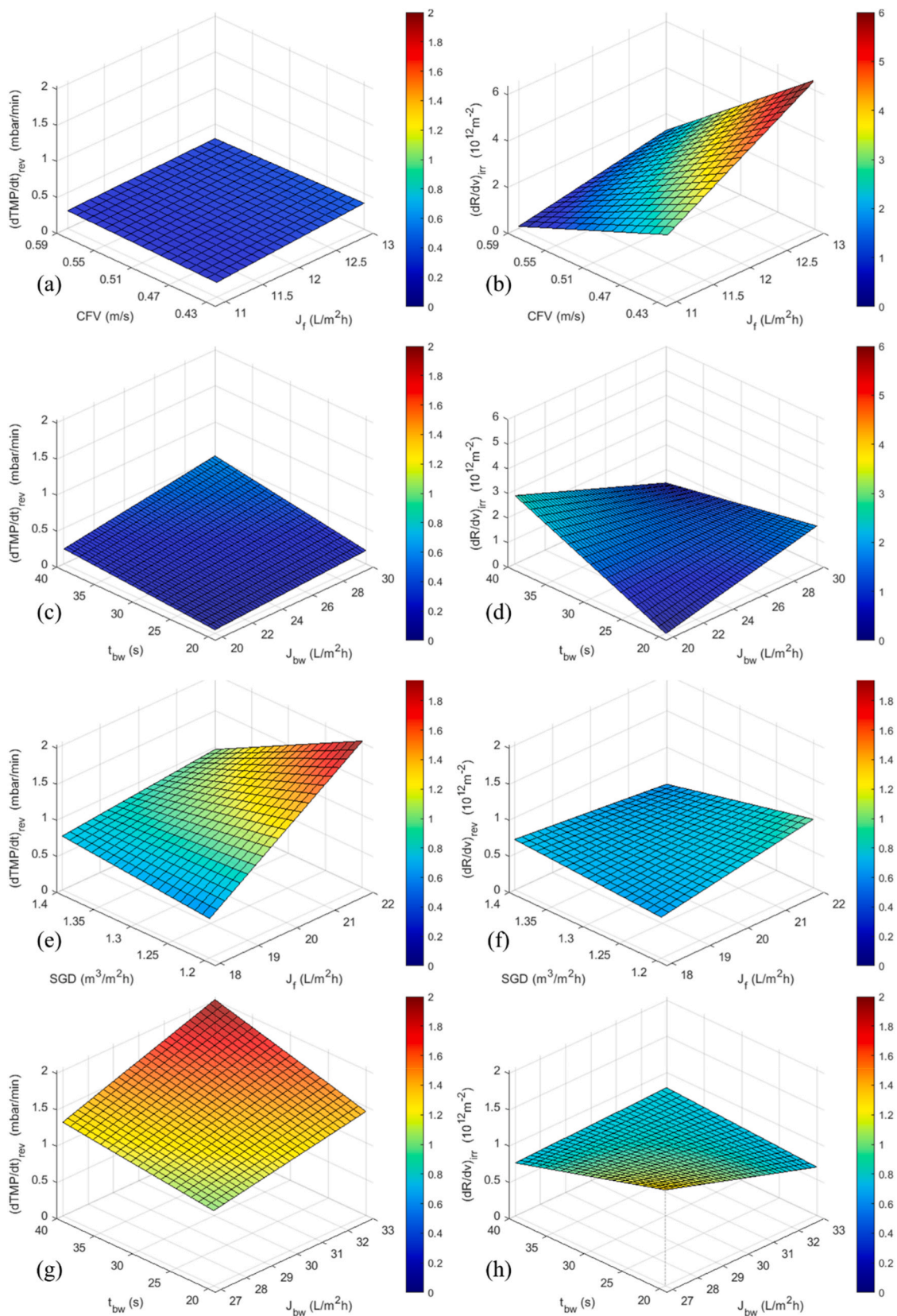The authors declare that they have no known competing financial

Fig. 5. Three-dimensional response surface of both the reversible, (dTMP/dt)$_{rev}$, and the irreversible (dR$_0$/dv)$_{irr}$, fouling rates. Box-Behnken design performed with the external membrane AE: (a) reversible and (b) irreversible fouling rate; Box-Behnken design BE: (c) reversible and (d) irreversible fouling rate; Box-Behnken designs perfomed with the submerged membrane AS: (e) reversible and (f) irreversible fouling rate; Box-Behnken design BS: (g) reversible and (h) irreversible fouling rate. All the response surfaces correspond to a cycle duration of 15 min and, in the case of (a) and (b), to a specific gas demand of 1.3 m^3/m^{2}h.

interests or personal relationships that could have appeared to influence the work reported in this paper.

Acknowledgements

References

Abuabdou, S.M.A., Ahmad, W., Aun, N.C., Bashir, M.J.K., 2020. A review of anaerobic membrane bioreactors (AnMBR) for the treatment of highly contaminated landfill leachate and biogas production: effectiveness, limitations and future perspectives. J. Clean. Prod. 255, 120215. https://doi.org/10.1016/j.jclepro.2020.120215.

Andrade, L.H. de, Mendes, F.D., dos, S., Espindola, J.C., Amaral, M.C.S., 2014. Internal versus external submerged membrane bioreactor configurations for dairy wastewater treatment. Desalin. Water Treat. 52, 2920–2932. https://doi.org/10.1080/19443994.2013.799048.

Asif, M.B., Habib, R., Iftekhar, S., Khan, Z., Majeed, N., 2017. Optimization of the operational parameters in a submerged membrane bioreactor using Box Behnken response surface methodology: membrane fouling control and effluent quality. Desalin. Water Treat. 82, 26–38. https://doi.org/10.5004/dwt.2017.20998.

Box, G.E.P., Behnken, D.W., 1960. Some new three level designs for the study of quantitative variables. Technometrics 2, 455–475. https://doi.org/10.1080/00401706.1960.10489912.

Chang, I.-S., Le Clech, P., Jefferson, B., Judd, S., 2002. Membrane fouling in membrane bioreactors for wastewater treatment. J. Environ. Eng. 128, 1018–1029. https://doi.org/10.1061/(ASCE)0733-9372.

Christensen, M.L., Bugge, T.V., Hede, B.H., Nierychlo, M., Larsen, P., Jørgensen, M.K., 2016. Effects of relaxation time on fouling propensity in membrane bioreactors. J. Membr. Sci. 504, 176–184. https://doi.org/10.1016/j.memsci.2016.01.006.

Diez, V., Cámara, J.M., Ruiz, M.O., Martínez, R., Ramos, C., 2021. A novel jet-loop anaerobic filter membrane bioreactor treating raw slaughterhouse wastewater: biological and filtration processes. Chem. Eng. J. 408, 127288. https://doi.org/10.1016/j.cej.2020.127288.

Diez, V., Ramos, C., Cabezas, J.L., 2012. Treating wastewater with high oil and grease content using an Anaerobic Membrane Bioreactor (AnMBR). Filtration and cleaning assays. Water Sci. Technol. 65, 1847–1853. https://doi.org/10.2166/wst.2012.852.

Drews, A., 2010. Membrane fouling in membrane bioreactors-Characterisation, contradictions, cause and cures. J. Membr. Sci. 363, 1–28. https://doi.org/10.1016/j.memsci.2010.06.046.

Foley, G., 2006. A review of factors affecting filter cake properties in dead-end microfiltration of microbial suspensions. J. Membr. Sci. 274, 38–46. https://doi.org/10.1016/j.memsci.2005.12.008.

Fu, H.Y., Xu, P.C., Huang, G.H., Chai, T., Hou, M., Gao, P.F., 2012. Effects of aeration parameters on effluent quality and membrane fouling in a submerged membrane bioreactor using Box–Behnken response surface methodology. Desalination 302, 33–42. https://doi.org/10.1016/J.DESAL.2012.06.018.

González, E., Díaz, O., Vera, L., Rodríguez-Gómez, L.E., Rodríguez-Sevilla, J., 2018. Feedback control system for filtration optimisation based on a simple fouling model dynamically applied to membrane bioreactors. J. Membr. Sci. 552, 243–252. https://doi.org/10.1016/j.memsci.2018.02.007.

Huang, Z., Liu, J., Liu, Y., Xu, Y., Li, R., Hong, H., Shen, L., Lin, H., Liao, B.Q., 2021. Enhanced permeability and antifouling performance of polyether sulfone (PES) membrane via elevating magnetic Ni@MXene nanoparticles to upper layer in phase inversion process. J. Membr. Sci. 623, 119080. https://doi.org/10.1016/j.memsci.2021.119080.

Huber, P.J., 1973. Robust regression: asymptotics, conjectures and Monte Carlo. Ann. Stat. 1, 799–821.

Jeison, D., van Lier, J.B., 2007. Cake formation and consolidation: main factors governing the applicable flux in anaerobic submerged membrane bioreactors (AnSMBR) treating acidified wastewaters. Separ. Purif. Technol. 56, 71–78. https://doi.org/10.1016/j.seppur.2007.01.022.

Jeison, D., van Lier, J.B., 2006. Cake layer formation in anaerobic submerged membrane bioreactors (AnSMBR) for wastewater treatment. J. Membr. Sci. 284, 227–236. https://doi.org/10.1016/j.memsci.2006.07.035.

Judd, S.J., Judd, C., 2011. The MBR Book: Principles and Applications of Membrane Bioreactors for Water and Wastewater Treatment, second ed. Elsevier.

Le-Clech, P., Jefferson, B., Judd, S.J., 2005. A comparison of submerged and sidestream tubular membrane bioreactor configurations. Desalination 173, 113–122. https://doi.org/10.1016/j.desal.2004.08.029.

Li, R., Rao, L., Zhang, J., Shen, L., Xu, Y., You, X., Liao, B.Q., Lin, H., 2021. Novel in-situ electroflotation driven by hydrogen evolution reaction (HER) with polypyrrole (PPy)-Ni-modified fabric membrane for efficient oil/water separation. J. Membr. Sci. 635, 119502. https://doi.org/10.1016/j.memsci.2021.119502.

Li, X., Yan, Wang, X, mao, 2006. Modelling of membrane fouling in a submerged membrane bioreactor. J. Membr. Sci. 278, 151–161. https://doi.org/10.1016/j.memsci.2005.10.051.

Liu, Z., Yu, J., Xiao, K., Chen, C., Ma, H., Liang, P., Zhang, X., Huang, X., 2020. Quantitative relationships for the impact of gas sparging conditions on membrane fouling in anaerobic membrane bioreactor. J. Clean. Prod. 276, 123139 https://doi.org/10.1016/j.jclepro.2020.123139.

Long, Y., Yu, G., Dong, L., Xu, Y., Lin, H., Deng, Y., You, X., Yang, L., Liao, B.Q., 2021. Synergistic fouling behaviors and mechanisms of calcium ions and polyaluminum chloride associated with alginate solution in coagulation-ultrafiltration (UF) process. Water Res. 189, 116665. https://doi.org/10.1016/J.WATRES.2020.116665.

Luo, J., Chen, W., Song, H., Liu, J., 2020. Antifouling behaviour of a photocatalytic modified membrane in a moving bed bioreactor for wastewater treatment. J. Clean. Prod. 256, 120381. https://doi.org/10.1016/j.jclepro.2020.120381.

Martínez, R., Ruiz, M.O., Ramos, C., Cámara, J.M., Diez, V., 2020. Comparison of external and submerged membranes used in anaerobic membrane bioreactors: fouling related issues and biological activity. Biochem. Eng. J. 159, 107558. https://doi.org/10.1016/j.bej.2020.107558.

Meng, F., Chae, S.R., Drews, A., Kraume, M., Shin, H.S., Yang, F., 2009. Recent advances in membrane bioreactors (MBRs): membrane fouling and membrane material. Water Res. 43, 1489–1512. https://doi.org/10.1016/j.watres.2008.12.044.

Nywening, J.P., Zhou, H., 2009. Influence of filtration conditions on membrane fouling and scouring aeration effectiveness in submerged membrane bioreactors to treat municipal wastewater. Water Res. 43, 3548–3558. https://doi.org/10.1016/j.watres.2009.04.050.

Pourabdollah, M., Torkian, A., Hosseinzadeh, M., 2016. A new approach to modeling operational conditions for mitigating fouling in membrane bioreactor. Water Environ. Res. 88, 2198–2208. https://doi.org/10.2175/106143016x14798353399133.

Prieto, A.L., Futselaar, H., Lens, P.N.L., Bair, R., Yeh, D.H., 2013. Development and start up of a gas-lift anaerobic membrane bioreactor (Gl-AnMBR) for conversion of sewage to energy, water and nutrients. J. Membr. Sci. 441, 158–167. https://doi.org/10.1016/j.memsci.2013.02.016.

Schoeberl, P., Brik, M., Bertoni, M., Braun, R., Fuchs, W., 2005. Optimization of operational parameters for a submerged membrane bioreactor treating dyehouse wastewater. Separ. Purif. Technol. 44, 61–68. https://doi.org/10.1016/j.seppur.2004.12.004.

Teng, J., Zhang, M., Leung, K.T., Chen, J., Hong, H., Lin, H., Liao, B.Q., 2019. A unified thermodynamic mechanism underlying fouling behaviors of soluble microbial products (SMPs) in a membrane bioreactor. Water Res. 149, 477–487. https://doi.org/10.1016/j.watres.2018.11.043.

Vera, L., González, E., Díaz, O., Sánchez, R., Bohorque, R., Rodríguez-Sevilla, J., 2015. Fouling analysis of a tertiary submerged membrane bioreactor operated in dead-end mode at high-fluxes. J. Membr. Sci. 493, 8–18. https://doi.org/10.1016/j.memsci.2015.06.014.

Vera, L., González, E., Ruigómez, I., Gómez, J., Delgado, S., 2016. Influence of gas sparging intermittence on ultrafiltration performance of anaerobic suspensions. Ind. Eng. Chem. Res. 55, 4668–4675. https://doi.org/10.1021/acs.iecr.5b04529.

Villarroel, R., Delgado, S., González, E., Morales, M., 2013. Physical cleaning initiation controlled by transmembrane pressure set-point in a submerged membrane bioreactor. Separ. Purif. Technol. 104, 55–63. https://doi.org/10.1016/j.seppur.2012.10.047.

Wazer, J.R. van, Lyons, J.W., Kim, K.Y., Colwell, R.E., Schierbauni, F., 1964. Viscosity and Flow Measurement. A Laboratory Handbook of Rheology, 1963. Interscience Publishers, a division of John Wiley and Sons, New York, London, pp. 371–372. https://doi.org/10.1002/star.19640161109. XX, 406 Seiten mit zahlreichen Abb. u. Tab.,. Starch - Stärke 16.

Wu, J., He, C., Zhang, Y., 2012. Modeling membrane fouling in a submerged membrane bioreactor by considering the role of solid, colloidal and soluble components. J. Membr. Sci. 102–111. https://doi.org/10.1016/j.memsci.2012.01.026, 397–398.

Wu, J., Le-Clech, P., Stuetz, R.M., Fane, A.G., Chen, V., 2008. Effects of relaxation and backwashing conditions on fouling in membrane bioreactor. J. Membr. Sci. 324, 26–32. https://doi.org/10.1016/j.memsci.2008.06.057.

Wu, M., Chen, Y., Lin, H., Zhao, L., Shen, L., Li, R., Xu, Y., Hong, H., He, Y., 2020. Membrane fouling caused by biological foams in a submerged membrane bioreactor: mechanism insights. Water Res. 181, 115932. https://doi.org/10.1016/j.watres.2020.115932.

Yang, Y., Bogler, A., Ronen, Z., Oron, G., Herzberg, M., Bernstein, R., 2020. Initial deposition and pioneering colonization on polymeric membranes of anaerobes isolated from an anaerobic membrane bioreactor (AnMBR). Environ. Sci. Technol. 54, 5832–5842. https://doi.org/10.1021/acs.est.9b06763.

Zhang, B., Huang, D., Shen, Y., Yin, W., Gao, X., Shi, W., 2020. Treatment of municipal wastewater with aerobic granular sludge membrane bioreactor (AGMBR): performance and membrane fouling. J. Clean. Prod. 273, 123124. https://doi.org/10.1016/j.jclepro.2020.123124.

Zhang, M., Hong, H., Lin, H., Shen, L., Yu, H., Ma, G., Chen, J., Liao, B.Q., 2018. Mechanistic insights into alginate fouling caused by calcium ions based on terahertz time-domain spectra analyses and DFT calculations. Water Res. 129, 337–346. https://doi.org/10.1016/j.watres.2017.11.034.

Zhang, W., Zhu, Z., Jaffrin, M.Y., Ding, L., 2014. Effects of hydraulic conditions on effluent quality, flux behavior, and energy consumption in a shear-enhanced membrane filtration using Box-Behnen response surface methodology. Ind. Eng. Chem. Res. 53, 7176–7185. https://doi.org/10.1021/ie500117u.

Zsirai, T., Aerts, P., Judd, S., 2013. Reproducibility and applicability of the flux step test for a hollow fibre membrane bioreactor. Separ. Purif. Technol. 107, 144–149. https://doi.org/10.1016/j.seppur.2013.01.027.

Zsirai, T., Buzatu, P., Aerts, P., Judd, S., 2012. Efficacy of relaxation, backflushing, chemical cleaning and clogging removal for an immersed hollow fibre membrane bioreactor. Water Res. 46, 4499–4507. https://doi.org/10.1016/j.watres.2012.05.004.